

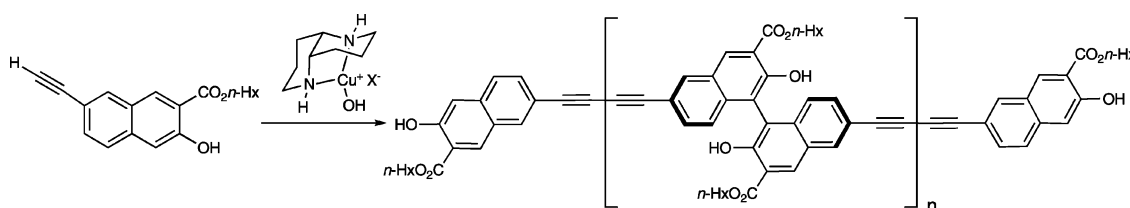
Enantioselective Synthesis of Binaphthyl Polymers Using Chiral Asymmetric Phenolic Coupling Catalysts: Oxidative Coupling and Tandem Glaser/Oxidative Coupling

Barbara J. Morgan, Xu Xie, Puay-Wah Phuan, and Marisa C. Kozlowski*

Department of Chemistry, Roy and Diana Vagelos Laboratories, University of Pennsylvania, Philadelphia, Pennsylvania 19104

marisa@sas.upenn.edu

Received April 3, 2007



A series of functionalized and optically active polybinaphthyls have been synthesized from *achiral* substrates by asymmetric oxidative phenolic coupling using a chiral 1,5-diaza-*cis*-decalin copper catalyst. In most cases, a copper tetrafluoroborate catalyst was found to be superior to the copper iodide catalyst, as *ortho*-iodination of the substrates could be prevented. Three methods for the formation of chiral polymers are described. In the first method, two 2-naphthols linked together at C-6 are subjected to the optimized asymmetric oxidative phenolic coupling conditions to form chiral polynaphthyls. A combination of NMR and HPLC measurements secured the selectivity of the asymmetric coupling. In the second method, substrates containing only one naphthalene were utilized. By incorporating a 2-naphthol and a terminal alkyne, the chiral copper catalysts effect both Glaser–Hay coupling of the alkyne and oxidative asymmetric coupling of the 2-naphthol with remarkable chemoselectivity. The relative reaction rates of various moieties with the chiral catalysts follows the order: benzyl cyanides \gg aryl alkynes $>$ electron-rich 2-naphthols $>$ electron-deficient 2-naphthols $>$ alkyl alkynes. Because of high chemoselectivity, this approach is useful for the organized assembly of multifunctional substrates in a single operation. In all cases, no cross-coupling is observed between the alkyne and the 2-naphthol. This approach was thus applied to a set of highly functionalized precursors. In this third case, the biaryl coupling was performed first and a Glaser–Hay coupling was performed in a separate step to generate a highly functionalized polymer. In some cases, the resultant chiral polymers exhibit very large optical rotations.

Introduction

Optically active polybinaphthyls are important chiral materials with high thermal and configurational stability. Typically, chiral polynaphthyls are polymerized at 2,2′-, 3,3′-, 4,4′-, and 6,6′-positions (Figure 1).¹ Potential applications for optically active polybinaphthyls include liquid crystalline materials, optically nonlinear materials, soluble high-temperature materials, electrochemical sensors, and polarized light emitters. For instance, the 6,6′-linked poly(arylenevinylene)-polynaphthyls exhibit higher fluorescence quantum yields relative to the racemic

version and high doped conductivity.² The 2,2′-linked polycarbonates-polynaphthyls have a stable helical conformation in solution.³ Optically active polybinaphthyls have also found utility as catalysts for asymmetric transformations.⁴ For example, several of the 3,3′-linked polymers display excellent enantio-

(1) For a review on polynaphthyls, see: Pu, L. *Chem. Rev.* **1998**, *98*, 2405–2494.

(2) (a) Hu, Q.; Vitharana, D.; Liu, G.; Jai, V.; Wagaman, M. W.; Zhang, L.; Lee, T. R.; Pu, L. *Macromolecules* **1996**, *29*, 1082–1084. (b) Tsubaki, K.; Miura, M.; Nakamura, A.; Kawabata, T. *Tetrahedron Lett.* **2006**, *47*, 1241–1244.

(3) (a) Hu, Q.; Huang, W.; Vitharana, D.; Zheng, X.; Pu, L. *J. Am. Chem. Soc.* **1997**, *119*, 12454–12464. (b) Pieraccini, S.; Ferrarino, A.; Fuji, K.; Gottarelli, G.; Lena, S.; Tsubaki, K.; Spada, G. P. *Chem. Eur. J.* **2006**, *12*, 1121–1126.

(4) For reviews see: (a) Pu, L. *Tetrahedron: Asymmetry* **1998**, *9*, 1457–1477. (b) Pu, L. *Chem. Eur. J.* **1999**, *5*, 2227–2232.

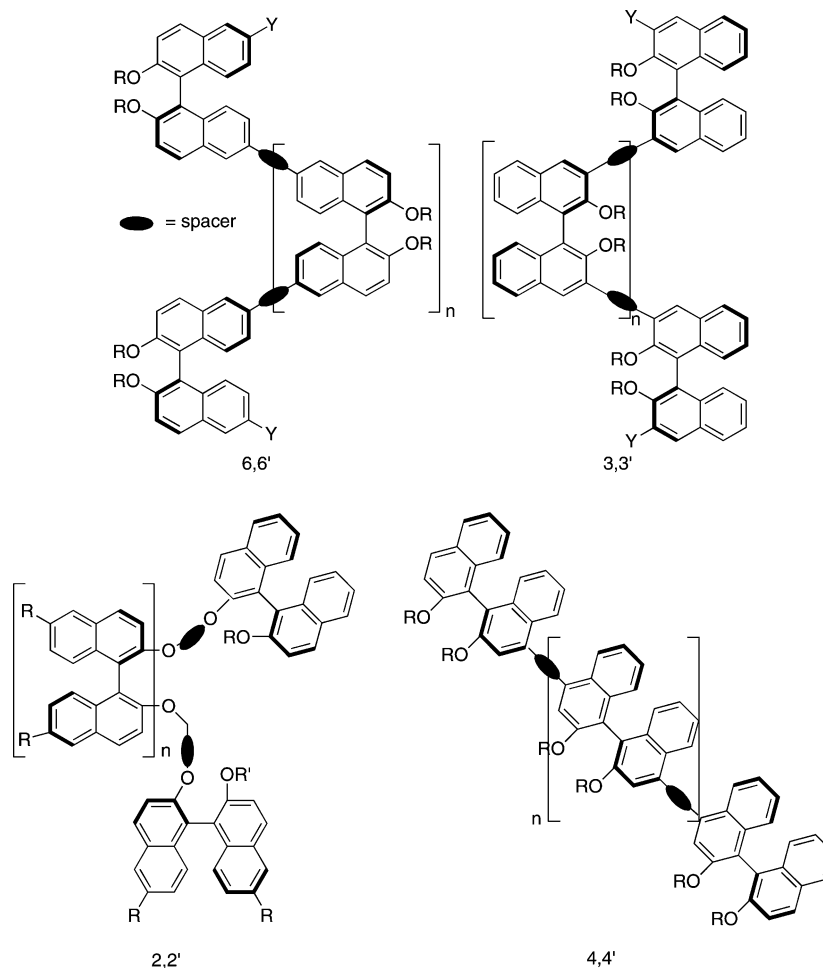


FIGURE 1. Chiral 1,1'-binaphthalene polymers derived from chiral monomers.

selectivity as catalyst in the asymmetric addition of Et_2Zn to a broad range of aldehydes.⁵ One advantage of the polymer catalysts is ready recovery and reuse without loss of selectivity. Because of the importance of chiral binaphthyls, many methods have been developed for the preparation: condensation of functionalized binaphthyl monomers,⁶ the polymerization of binaphthyls containing olefin groups,⁷ the ring-opening polymerization of binaphthyl carbonates,⁸ and transition metal-

catalyzed cross-couplings.⁹ Notably, the majority of the optically active polybinaphthyls reported have been made by polymerization of the optically active binaphthyl monomers.¹⁰

Because of the important properties that optically active polybinaphthyls exhibit as well as their successful application to asymmetric catalysis, the synthesis of binaphthyl polymers with different functionality and the development of new methods for more efficient polymerizations are important. The majority of prior reports of the preparation of chiral binaphthyl polymers begin with chiral 1,1'-binaphthyl monomers. Previously, we reported the first enantioselective synthesis of functionalized chiral polybinaphthyls from *achiral* starting materials.¹¹ Since then, other methods have been reported for the asymmetric

(5) (a) Huang, W.; Hu, Q.; Zheng, X.; Anderson, J.; Pu, L. *J. Am. Chem. Soc.* **1997**, *119*, 4313–4314. (b) Hu, Q.; Zheng, X.; Pu, L. *J. Org. Chem.* **1996**, *61*, 5200–5201. (c) Huang, W.; Hu, Q.; Pu, L. *J. Org. Chem.* **1998**, *63*, 1364–1365. (d) Hu, Q.; Huang, W.; Pu, L. *J. Org. Chem.* **1998**, *63*, 2798–2799. (e) Arai, T.; Hu, Q.; Zheng, X.; Pu, L.; Sasaki, H. *Org. Lett.* **2000**, *2*, 4261–4263. (f) Yu, H.; Hu, Q.; Pu, L. *J. Am. Chem. Soc.* **2000**, *122*, 6500–6501.

(6) (a) Schulz, R. C.; Jung, R. H. *Makromol. Chem.* **1968**, *116*, 190–202. (b) Tamai, Y.; Matsuzaka, Y.; Oi, S.; Miyano, S. *Bull. Chem. Soc. Jpn.* **1991**, *64*, 2260–2265. (c) Mi, Q.; Gao, L.; Ding, M. *Macromolecules* **1996**, *29*, 5758–5759.

(7) (a) Kakuchi, T.; Yokota, K. *Makromol. Chem. Rapid Commun.* **1985**, *6*, 551–555. (b) Kakuchi, T.; Sasaki, H.; Yokota, K. *Makromol. Chem.* **1988**, *189*, 1279–1285. (c) Yokota, K.; Kakuchi, T.; Sasaki, H.; Ohmori, H. *Makromol. Chem.* **1989**, *190*, 1269–1275. (d) Yokota, K.; Kakuchi, T.; Yamamoto, T.; Hasegawa, T.; Haba, O. *Makromol. Chem.* **1992**, *193*, 1805–1813. (e) Kakuchi, T.; Hasegawa, T.; Sasaki, H.; Ohmori, H.; Yamaguchi, K.; Yokota, K. *Makromol. Chem.* **1989**, *190*, 2091–2097. (f) Nakano, T.; Sogah, D. Y. *J. Am. Chem. Soc.* **1995**, *117*, 534–535. (g) Puts, R. D.; Sogah, D. Y. *Macromolecules* **1995**, *28*, 390–392.

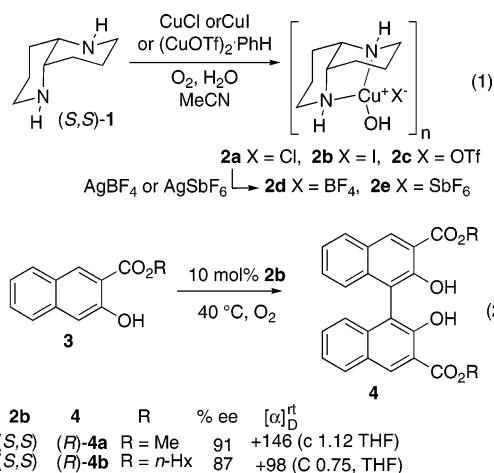
(8) (a) Takata, T.; Furusho, Y.; Murakawa, K.-i.; Endo, T.; Matsuoka, H.; Hirasa, T.; Matsuo, J.; Sisido, M. *J. Am. Chem. Soc.* **1998**, *120*, 4530–4531. (b) Tanaka, T.; Matsuoka, H.; Endo, T. *Chem. Lett.* **1991**, 2091–2094.

(9) (a) Bedworth, P. W.; Tour, J. M. *Macromolecules* **1994**, *27*, 622–624. (b) Hu, Q.; Vitharana, D. R.; Pu, L. In *Electrical, Optical, and Magnetic Properties of Organic Solid State Materials III*; Jen, A. K.-Y., Lee, C. Y.-C., Dalton, L. R., Rubner, M. F., Wnek, G. E., Chiang, L. Y., Eds.; MRS: Pittsburgh, 1996; p 621. (c) Ma, L.; Hu, Q.-S.; Musick, K.; Vitharana, D. R.; Wu, C.; Kwan, C. M. S.; Pu, L. *Macromolecules* **1996**, *29*, 5083–5090. (d) Ma, L.; Hu, Q.-S.; Pu, L. *Tetrahedron: Asymmetry* **1996**, *7*, 3103–3106. (e) Cheng, H.; Ma, L.; Hu, Q.; Zheng, X.; Anderson, J.; Pu, L. *Tetrahedron: Asymmetry* **1996**, *7*, 3083–3086. (f) Hu, Q.; Vitharana, D. R.; Liu, G.; Jain, V.; Pu, L. *Macromolecules* **1996**, *29*, 5075–5082. (g) Huang, W. S.; Hu, Q.-S.; Zheng, X. F.; Anderson, J.; Pu, L. *J. Am. Chem. Soc.* **1997**, *119*, 4313–4314. (h) Song, J.; Cheng, Y.; Chen, L.; Zou, X.; Zhiliu, W. *Eur. Polym. J.* **2006**, *42*, 663–669.

(10) Examples of polymerizations via diastereoselective oxidative biaryl couplings of chiral BINOL derivatives have been reported: (a) Habaue, S.; Seko, T.; Okamoto, Y. *Macromolecules* **2002**, *35*, 2437–2439. (b) Habaue, S.; Seko, T.; Isonaga, M.; Ajiro, H.; Okamoto, Y. *Polym. J.* **2003**, *35*, 592–597.

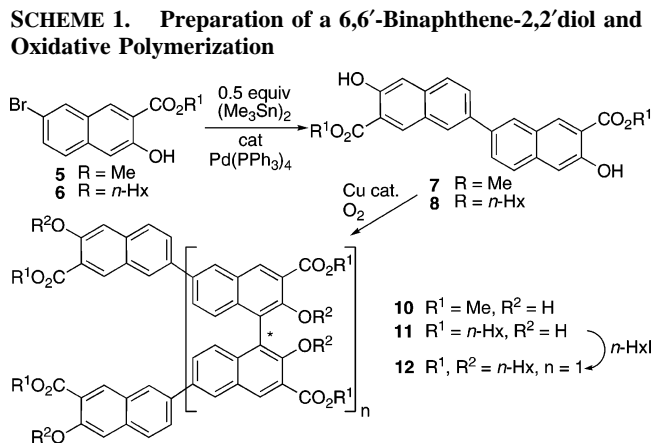
polymerization of naphthalene units, but most processes resulted in low to moderate yields and enantioselectivities.¹² The stereoselective polymerization of chiral binaphthalene derivatives as a monomeric unit has also been reported recently, where the polymerizations proceed under ligand control regardless of the monomer stereostructure.¹³ In addition, optically active polymers have been synthesized in high diastereoselectivity via second-order asymmetric transformations of chiral oligonaphthalene derivatives (from dimer to hexadecamer) as a monomeric unit.¹⁴

Overall, asymmetric C–C bond forming catalysis has proven efficient for the synthesis of optically active small molecules but has been utilized less frequently in asymmetric polymerizations.¹⁵ We have developed an efficient method to prepare chiral 1,1'-binaphthols utilizing 1,5-diaza-*cis*-decalin copper complexes such as **2** (eq 1) for the oxidative coupling of 2-naphthol derivatives (eq 2; 85% yield, 93% ee).¹⁶ Herein, we disclose the full results from our investigation of these copper catalysts in the asymmetric polymerization of achiral 2-naphthol compounds.



Results and Discussion

Asymmetric Polymerization of Naphthol Dimers. The polymerization precursors **7** and **8** were efficiently prepared from the corresponding 6-bromonaphthoate with hexamethylditin and catalytic Pd(PPh₃)₄ (Scheme 1). In this novel one-pot procedure,



both stannylation and cross-coupling are effected.¹⁷ With methyl ester monomer **7** in hand, this material was treated with the CuCl(OH)TMEDA (**9**) complex to afford a yellow solid **10** (Table 1, entry 1). Although **10** was not soluble in organic solvents, the corresponding acid was soluble in basic aqueous solutions. However, the ¹H NMR signals in D₂O/NaOD remained broadened and detailed structural information could not be obtained. To increase solubility, we turned to the *n*-hexyl ester analogue **8** which was prepared in the same manner as **7**. Application of the achiral CuCl(OH)TMEDA catalyst to **8** (Table 1, entry 2) yielded two fractions after column chromatography, **11a** and **11b**, with different molecular weight distributions as judged by GPC (*M*_w = 4800, *M*_n = 3100 vs *M*_w = 8500, *M*_n = 5800). From the ¹H NMR spectra, two sets of aromatic peaks were identified in both **11a** and **11b** which correspond to the internal repeat units and the termini units, respectively. The number average molecular weights (*M*_n) deduced from the NMR integrations correlated with the GPC data. To achieve a higher degree of polymerization, **8** was treated with the same catalyst at 80 °C. A jellylike material was obtained, and the soluble fraction contained only one set of aromatic peaks, indicating a higher degree of polymerization (>20:1 internal:terminal).

When **8** was subjected to polymerization with the CuI 1,5-diaza-*cis*-decalin catalysts (*R,R*)-**2b** and (*S,S*)-**2b** under similar conditions, a slight lower molecular weight **11c** was obtained (Table 1, entries 3 and 4). The optical rotations of **11c** from the two enantiomeric catalysts were comparable and of the opposite sign. Interestingly, the sign of the optical rotation of polymer (*R*)-**11c** (–73) is opposite that of the isolated binaphthyl unit (*R*)-**4b** (+101, eq 1). In other studies, similar phenomenon have been observed and attributed to the countervailing higher order structure of the polymeric form.^{7,18} However, the sign of the optical rotation of the *dimer* from **8**, (*R*)-**11e** (–60) is the same as that of polymer (*R*)-**11c** (–73). We believe that this type of comparison is more valid, as the polymer end groups are present in dimer **11e** but not in **4b**. Thus, the higher order structure in polymer **11c** does not reverse the optical rotation. Unfortunately, purification of **11c** was complicated by the formation of byproducts. We speculated that these byproducts arose from

(11) Xie, X.; Phuan, P.-W.; Kozłowski, M. *Angew. Chem., Int. Ed.* **2003**, *42*, 2168–2170.

(12) (a) Habaue, S.; Seko, T.; Okamoto, Y. *Macromolecules* **2003**, *36*, 2604–2608. (b) Habaue, S.; Murakami, S.; Higashimura, H. *J. Polym. Sci.: Part A: Polym. Chem.* **2005**, *43*, 5872–5878.

(13) Habaue, S.; Ajiro, H.; Yoshii, Y.; Hirasa, T. *J. Polym. Sci.: Part A: Polym. Chem.* **2004**, *42*, 4528–4534.

(14) (a) Tsubaki, K.; Miura, M.; Morikawa, H.; Tanaka, H.; Kawabata, T.; Furuta, T.; Tanaka, K.; Fuji, K. *J. Am. Chem. Soc.* **2003**, *125*, 16200–16201. (b) Tsubaki, K.; Tanaka, H.; Takashi, K.; Miura, M.; Morikawa, H.; Furuta, T.; Tanaka, K.; Fuji, K.; Sasamori, T.; Tokitoh, N.; Kawabata, T. *J. Org. Chem.* **2006**, *71*, 6579–6587.

(15) For some examples of asymmetric polymerization: (a) Coates, G.; Waymouth, R. M. *J. Am. Chem. Soc.* **1993**, *115*, 91–98. (b) Brookhart, M.; Wagner, M. I. *J. Am. Chem. Soc.* **1994**, *116*, 3641–3642. (c) Nozaki, K.; Sato, N.; Tomomura, Y.; Yasutomi, M.; Takaya, H.; Hiyama, T.; Matsubara, T.; Koga, N. *J. Am. Chem. Soc.* **1997**, *119*, 12779–12795. (d) Kenichi, K.; Itsuno, S.; Ito, K. *Chem. Commun.* **1999**, 35–36. (e) Nozaki, K.; Kawashima, Y.; Oda, T.; Hiyama, T. *Macromolecules* **2002**, *35*, 1140–1142.

(16) Li, X.; Yang, J.; Kozłowski, M. C. *Org. Lett.* **2001**, *3*, 1137–1140.

(17) For related biaryl coupling see: (a) Grigg, R.; Teasdale, A.; Sridharan, V. *Tetrahedron Lett.* **1991**, *32*, 3859–3862. (b) Kelly, T. R.; Li, Q.; Bhushan, V. *Tetrahedron Lett.* **1990**, *31*, 161–164.

(18) For similar structural effects with related polybinaphthyls, see: (a) Wyatt, S. R.; Hu, Q.-S.; Yan, X.-L.; Bare, W. D.; Pu, L. *Macromolecules* **2001**, *34*, 7983–7988. (b) Ma, L.; White, P. S.; Lin, W. *J. Org. Chem.* **2002**, *67*, 7577–7586.

TABLE 1. Treatment of **7** and **8** with Selected Copper Catalysts (Scheme 1)

entry	R ¹	catalyst		time	T (°C)	products	yield, %	M _w ^a	M _n ^a	M _w /M _n ^a	[α] _D ²⁵	int:term	
		mol %	no.									GPC ^a	NMR
1	Me		9	4 d	40	10					NA		
2	<i>n</i> -Hx	10	9	4 d	40	11a	37	4800	3100	1.6	NA	4.7:1	4.5:1
						11b	25	8500	5800	1.5	NA	9.6:1	9:1
3	<i>n</i> -Hx	10	(<i>R,R</i>)- 2b	4 d	40	(<i>S</i>) _n - 11c	52	2800	2200	1.3	+82	3.1:1	2.3:1
4	<i>n</i> -Hx	10	(<i>S,S</i>)- 2b	4 d	40	(<i>R</i>) _n - 11c	50	2600	2100	1.2	-73	2.9:1	2.4:1
5	<i>n</i> -Hx	10	(<i>R,R</i>)- 2d	5 d	60	(<i>S</i>) _n - 11d	74	10 500	4900	2.1	+78	8.1:1	>20:1
6	<i>n</i> -Hx	20	(<i>S,S</i>)- 2d	2 d	80	(<i>R</i>) _n - 11d	78	12 300	5400	2.3	-89	8.9:1	>20:1
7	<i>n</i> -Hx	10	9	1 h	60	11e (<i>n</i> = 1)	28				NA	NA	1:1
						11f (<i>n</i> = 2)	9				NA	NA	2:1
8	<i>n</i> -Hx	10	(<i>R,R</i>)- 2d	1 d	60	(<i>S</i>)- 11e (<i>n</i> = 1)	11				+50	NA	1:2
						(<i>S,S</i>)- 11f (<i>n</i> = 2)	7				+69	NA	2:1
9	<i>n</i> -Hx	10	(<i>S,S</i>)- 2d	3 h	60	(<i>R</i>)- 11e (<i>n</i> = 1)	31				-60	NA	1:1
						(<i>R,R</i>)- 11f (<i>n</i> = 2)	7				-71	NA	2:1

^a Measured by gel permeation chromatography (GPC) using a polystyrene standard.

ortho-iodination of **8** by the iodide present in catalyst **2b**. As such, we explored other catalysts (**2c–e**), which do not contain a halide counterion. Catalysts **2d,e** were readily generated from the chloride precursor **2a** via exchange with the corresponding silver(I) salt (eq 1). It was necessary to carry out the counterion exchange with the Cu(II) oxidation state, since the Cu(I) adducts with 1,5-diaza-*cis*-decalin underwent oxidation when treated with Ag(I) salts because of Ag(I) → Ag(0) redox chemistry.

The CuOTf, CuBF₄, and CuSbF₆ complexes **2c–e** all catalyze the dimerization of **3a** (eq 2) with enantioselectivity (89–94% ee) similar to the CuI complex **2b**. In addition, the byproducts observed with **2b** were eliminated with **2c–e**. The rates with the different catalysts did vary considerably (Figure 2). Both the CuOTf and CuSbF₆ catalysts were relatively slow. While the CuBF₄ catalyst is slightly slower initially than the CuI catalyst, the CuBF₄ catalyst ultimately forms **4a** to a greater extent since *ortho*-halogenation does not compete.

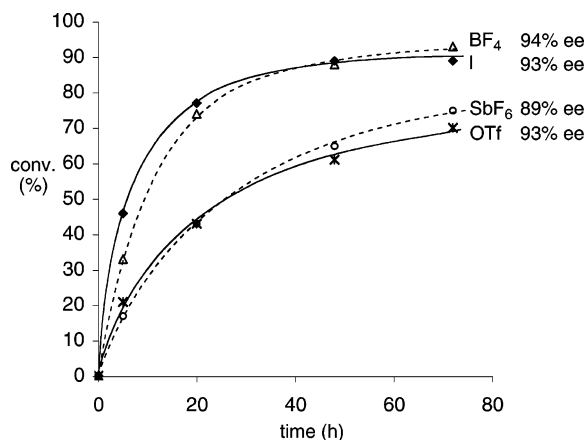
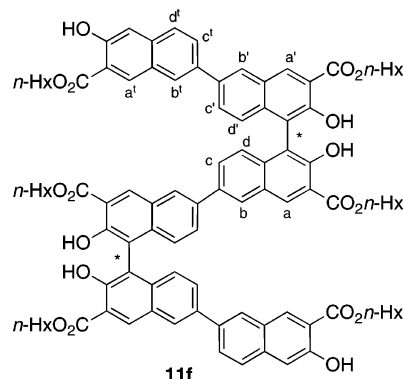


FIGURE 2. Rate profiles for catalyst **2b–e** (eq 1) in the formation of **4a** (eq 2).

With the optimal catalyst in hand, **8** was again subjected to polymerization (Table 1, entries 5–6). Not only was the yield (74–78%) of polymerized material (**11d**) higher, but the degree of polymerization was also higher ($M_w = 10\,500$ – $12\,300$, $M_n = 4900$ – 5400). The optical rotations of **11d** from the two enantiomeric catalysts again were approximately the same magnitude but of opposite signs indicating that chiral polymers were indeed being formed.

To determine the degree of asymmetric induction introduced in these polymerizations, **8** was treated with (*S,S*)-**2d** under milder conditions (Table 1, entry 9) to provide a mixture of recovered **8** (46%), dimer (*R*)-**11e** (*n* = 1, 31%), and trimer (*R*)-**11f** (*n* = 2, 7%) after chromatography. Similarly, racemic dimer **11e** and trimer **11f** were prepared by treating of **8** with CuCl(OH)TMEDA under milder conditions (Table 1, entry 7). HPLC analysis (Chiralpak AD) of the corresponding *n*-hexyl ethers **12** (Scheme 1) indicated that dimer (*R*)-**11e** was formed with 85% ee which is similar to the selectivity observed for **4b** (87% ee, eq 2). While HPLC resolution of the corresponding trimer, **11f**, was not possible, the ¹H NMR spectra of the trimer permitted assignment of the diastereomeric excess. Different values were observed for the chemical shifts of the internal aromatic protons of the diastereomers of **11f** (a–d and a'–d', Figure 3 and Figure 4). From integration of these signals, a 70–75% diastereomeric excess is measured for the trimer **11f** formed from (*S,S*)-**2d**. An 85% ee in each biaryl coupling would give a 72% de [85.5% (*R,R*)-**11f**, 14.0% (*S,R*)-**11f**, 0.5% (*S,S*)-**11f**] consistent with this NMR measurement. On this basis, it appears that each biaryl coupling in the polymerization proceeds *independently* with 85% ee and that an optically active polymer is formed when chiral **2d** is employed.



de calculated from the 85% ee of dimer **11e** = 72%
85.5% (*R,R*), 14.0% (*S,R*), 0.5% (*S,S*)

de measured from the NMR of trimer **11f** = 70%

FIGURE 3. ¹H NMR patterns which allow differentiation of (*R,R*)- and (*S,S*)-**11f** from (*S,R*)-**11f** (see Figure 4).

The CD and UV spectra of the dimers and trimers derived from **11** are shown in Figures 5 and 6. The UV spectra of the

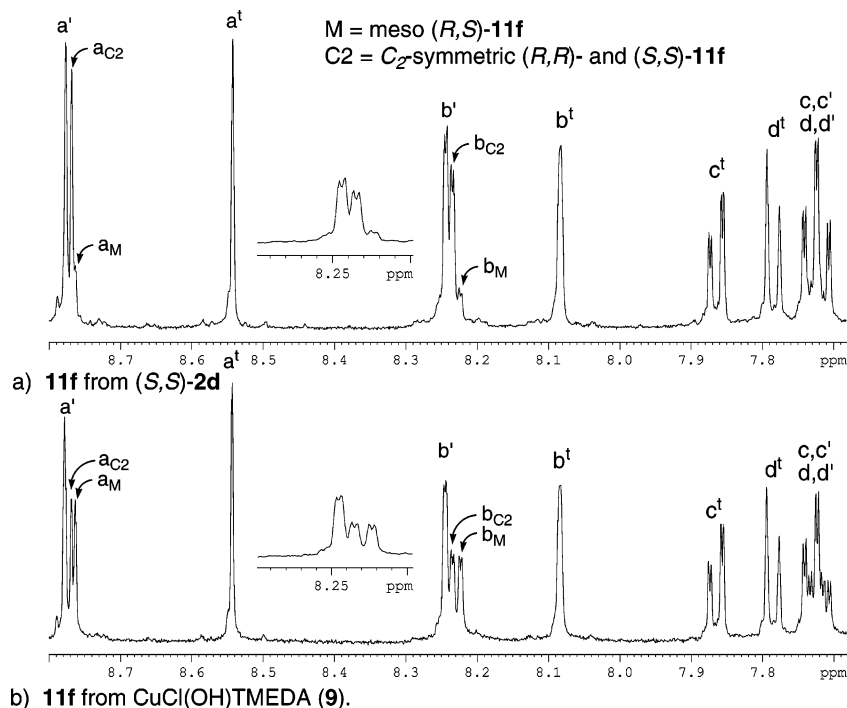


FIGURE 4. ^1H NMR spectra of the trimer **11f** generated from (*S,S*)-**2d** and from $\text{CuCl}(\text{OH})\text{TMEDA}$ (**9**).

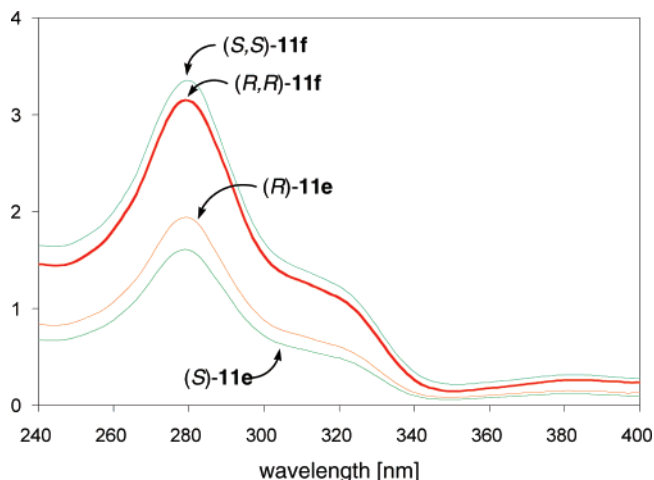


FIGURE 5. UV spectra of 1.7×10^{-4} M (*R*)-**11e**, (*R,R*)-**11f**, (*S*)-**11e**, and (*S,S*)-**11f**, in CH_2Cl_2 at ambient temperature.

dimer **11e** and trimer **11f** are very similar (same maxima and minima) except for a more intense signal due to the greater number of naphthalenes¹⁸ (Figure 5). The CD spectra of the enantiomeric dimers (**11e**) and trimers (**11f**) show mirror Cotton effects (Figure 6). Upon generation of dimer (*S*)-**11e** and the trimer (*S,S*)-**11f** under the conditions in entry 8 of Table 1, additional oligomeric material was observed (*S*)_n-**11d**. The CD spectra of the polymers **11d** from the enantiomeric catalysts also displayed a mirror Cotton effect except for a more intense signal.

Tandem Glaser–Hay Coupling and Asymmetric Oxidative Coupling. Typically, the main chain poly-1,1'-binaphthyls are polymerized via the 2,2',-⁵⁻⁸ 3,3',-^{19,4} 4,4',-^{9a} and 6,6'^{9b-9f}-positions. In prior reports and the work described above, the polybinaphthyls are formed from “monomer” units in which

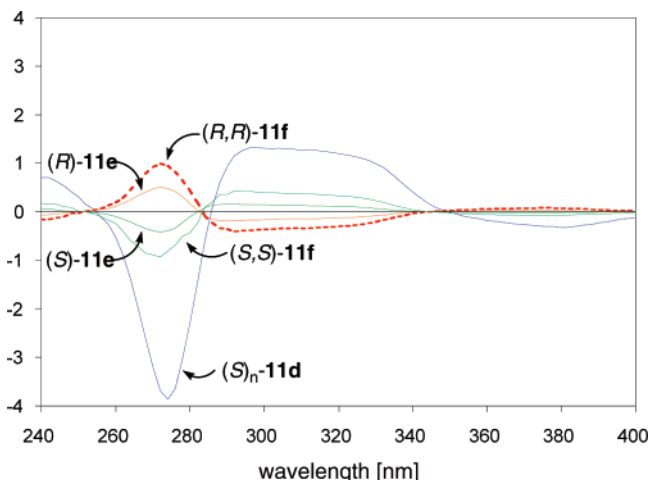


FIGURE 6. CD spectra of (*R*)-**11e**, (*R,R*)-**11f**, (*S*)-**11e**, (*S,S*)-**11f**, and (*S*)_n-**11d** in CH_2Cl_2 at ambient temperature. 1.7×10^{-4} M except (*S*)_n-**11d** which was 1.7×10^{-5} M.

one set of these linkages is already formed. A more efficient method for preparing such polymers would be to form *both* sets of linkages at the same time from monomers containing two sites, which react in the presence of copper oxidants. We proposed monomers **14** and **15** (eq 3, eq 4) as suitable for this purpose since each compound contains two sites that can react in the presence of copper oxidants, the alkyne terminus and C1 of the 2-naphthol. The self-reactivity of each site is high and the cross-reactivity is low, enabling formation of a well-defined polymer chain. The alkyne containing monomers **14** and **15** are

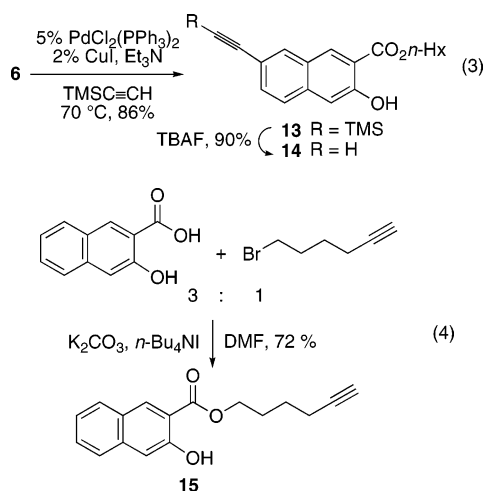
(19) (a) Li, C.-J.; Slaven, W. T.; IV.; John, V. T.; Banerjee, S. *J. Chem. Soc., Chem. Commun.* **1997**, 1569–1570. (b) Li, C.-J.; Wang, D.; Slaven, W. T., IV. *Tetrahedron Lett.* **1996**, 37, 4459–4462.

TABLE 2. Treatment of 14–16, 19 with Selected Copper Catalysts

entry	SM	catalyst		time	T (°C)	products	yield, %	M_w	M_n	M_w/M_n	$[\alpha]_D^{25}$	int:ter m	
		mol %	no.									GPC ^a	NMR
1	14	10	9	3 d	rt	16	77				NA		
2	16	20	(<i>S,S</i>)- 2d	2 d	80	(<i>R</i>) _{<i>n</i>} - 17a	90	12 900	4400	2.9	-248	6.4:1	5.7:1
3	14	20	(<i>S,S</i>)- 2d	2 d	80	(<i>R</i>) _{<i>n</i>} - 17b	80	9200	4900	1.9	-168	7.3:1	5.6:1
4	14	20	(<i>R,R</i>)- 2d	2 d	80	(<i>S</i>) _{<i>n</i>} - 17b	86	15 100	6800	2.2	+174	10.5: 1	9.1:1
5	19	10	9	2 d	80	(<i>S</i>) _{<i>n</i>} - 17c	86	11 000	5100	2.2	+238	7.6:1	7.4:1
6	15	10	9	2 d	rt	20	61				NA		
7	15	20	(<i>R,R</i>)- 2d	4 d	70	(<i>S</i>) _{<i>n</i>} - 21	60	10 300	3900	2.6	-180	6.3:1	NA

^a Measured by gel permeation chromatography (GPC) using a polystyrene standard.

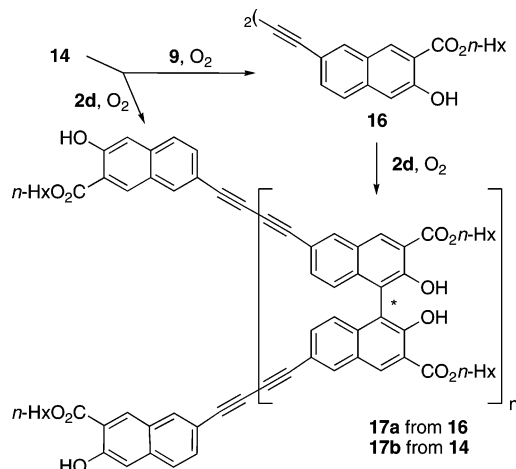
readily prepared from bromonaphthoate **6** (eq 3) and 3-hydroxy-2-naphthoic acid (eq 4), respectively.



Upon treatment of **14** with 10 mol % of the achiral CuCl(OH)TMEDA catalyst at room temperature, the Glaser–Hay coupling²⁰ was found to occur very rapidly resulting in formation of bisalkyne **16** in good yield (77%) (Scheme 2, Table 2, entry 1). Further reaction via phenolic coupling was accomplished by subjecting bisalkyne **16** to 20 mol % (*S,S*)-**2d** at 80 °C for 2 d to provide polymer (*R*)_{*n*}-**17a** in 90% yield. When monomer **14** was subjected to these same conditions (Table 2, entry 3), the material obtained, (*R*)_{*n*}-**17b**, was very similar to the (*R*)_{*n*}-**17a** obtained from **16** (Table 2, entry 2). Thus, we conclude that the polymerization occurs via tandem alkynyl and phenolic couplings. When the enantiomeric (*R,R*)-**2d** catalyst was employed with **14**, the enantiomeric polymer (*S*)_{*n*}-**17b** was observed (Table 2, entry 4). These enantiomeric polymers exhibit comparable optical rotations of opposite signs (-168 and 174), which are only slightly lower than that of **17a** (-248).

The UV and CD spectra of polymer **17** generated from **14** or **16** were identical (Figure 7 and Figure 8), indicating that catalyst **2d** can effect both the alkynyl and phenolic coupling cleanly. No cross-coupling and *no interference* by alkynyl copper intermediates on the stereochemical course of the biaryl coupling was observed.

In order to determine the stereochemical fidelity in the polymerization of **14** to **17**, silylated substrate **13** was examined in the oxidative biaryl coupling (Scheme 3). With the same CuBF₄ catalyst used in the polymerizations, **18** was obtained with 73% ee. Since the alkyne spacer units of **16** essentially

SCHEME 2. Sequential and Tandem Glaser–Hay Coupling/Oxidative Coupling from Alkynyl Naphthol **14**

isolate each biaryl coupling site, we infer that a similar level of enantioselectivity is exercised at each biaryl coupling during the polymerization resulting in an optically active polymer.

Furthermore, the silyl group of **18** was removed to produce the terminal alkyne **19** which was subjected to 10 mol % CuCl(OH)TMEDA to obtain the polymer **17c** with identical optical rotation as **17b** (Scheme 3, Table 2, entry 5). As both the UV and CD spectra support, the structure of the resultant product was identical to that of polymer **17** from **14** or **16** (Figure 7 and Figure 8) even though the termini are alkynyl instead of naphthalenyl. Therefore, we deduce that the one-pot asymmetric polymerizations from **14** were accomplished with ~73% ee.

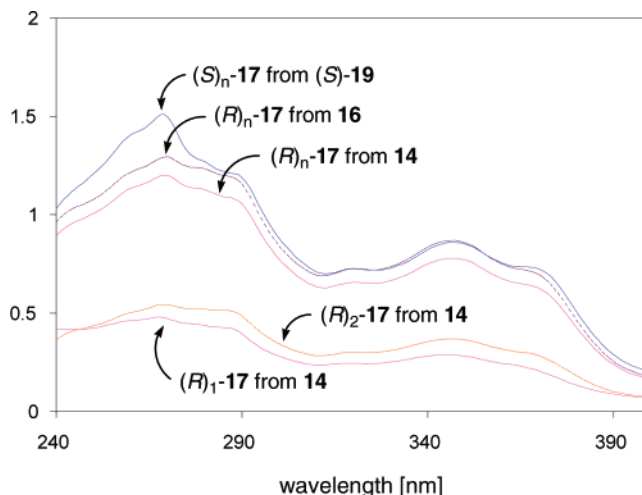


FIGURE 7. UV spectra of 2×10^{-5} M **9** in CH₂Cl₂ at ambient temperature.

(20) For, a review see: Siemsen, P.; Livingston, R. C.; Diederich, R. *F. Angew. Chem., Int. Ed.* **2000**, *39*, 2632–2657.

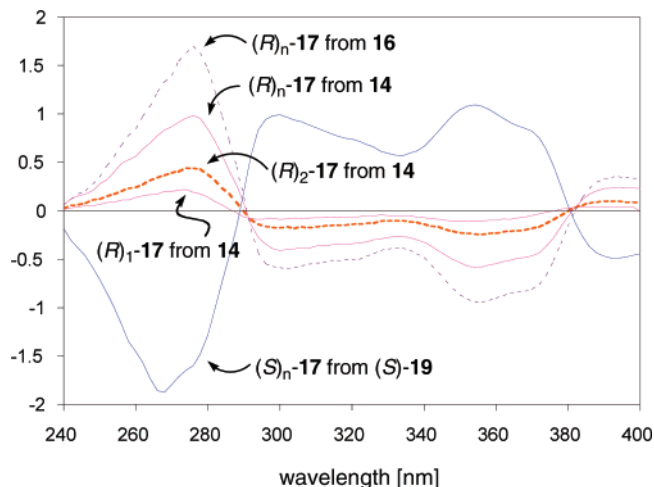
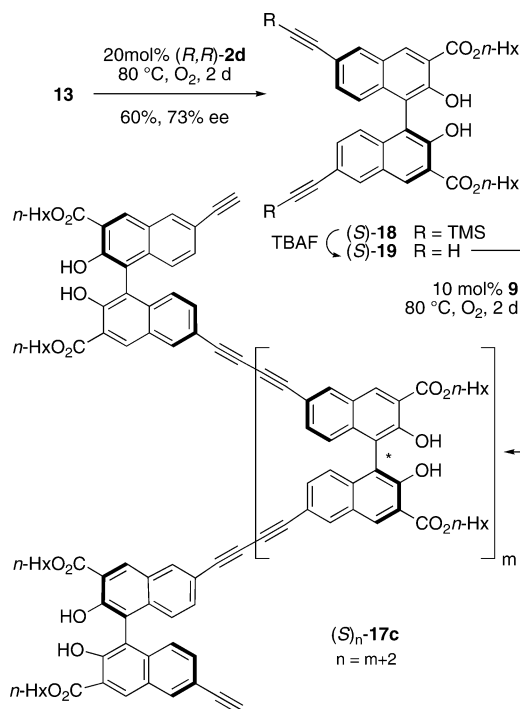


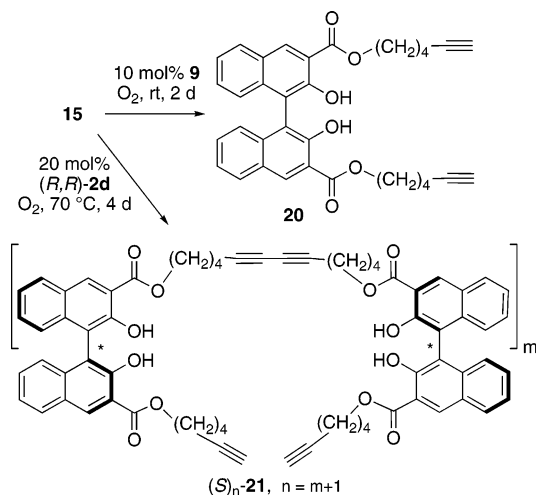
FIGURE 8. CD spectra of 2×10^{-5} M **9** in CH_2Cl_2 at ambient temperature.

SCHEME 3. Stepwise Oxidative Coupling and Glaser–Hay Coupling from Alkynyl Naphthol **13**



Surprisingly, when the other alkyne monomer **15**, with the alkyne attached via C3 ester instead of the directly to the naphthalene as in **14**, was subjected to the same conditions (10 mol % $\text{CuCl}(\text{OH})\text{TMEDA}$), the phenolic coupling occurred first to provide the biaryl coupling product **20** (61%) along with recovering starting material (15%) (Scheme 4, Table 2, entry 6). From this experiment we conclude that the rate of Glaser–Hay coupling for aryl-substituted alkynes is greater than that of alkyl-substituted alkynes and the rate of oxidative phenolic coupling of 3-carboxy-2-naphthols is intermediate to these two rates. Regardless of the relative rates, the chemoselectivity of each coupling is remarkably high and to date we have not observed any of the cross-coupled materials. The polymer of the alkynyl ester monomer **15**, (*S*)-**21**, could be prepared directly by subjecting monomer **15** to 20 mol % (*R,R*)-**2d** under more forcing conditions (Scheme 4, Table 2, entry 7). Interestingly,

SCHEME 4. Tandem Oxidative Coupling/Glaser–Hay Coupling to Generate Polynaphthols with 1,1'- and 3,3'-Linkages **4. Synthesis of a Highly Functionalized Naphthol**



the optical rotation of polymer (*S*)-**21** is negative while the optical rotation of the related polymer (*S*)-**17** (Scheme 3) is positive (Table 2). Even though both compounds possess the same binaphthol configurations, as they were prepared from the same chiral catalyst, the overall polymer architectures are substantially different.

The CD and UV spectra of the dimer and oligomers derived from **15** are shown in Figures 9 and 10. The spectra of the dimer (*S*)₁-**21** and oligomer (*S*)_n-**21** are very similar (same maxima and minima) except for a more intense signal due to the greater number of naphthalenes, indicating no higher order structure.

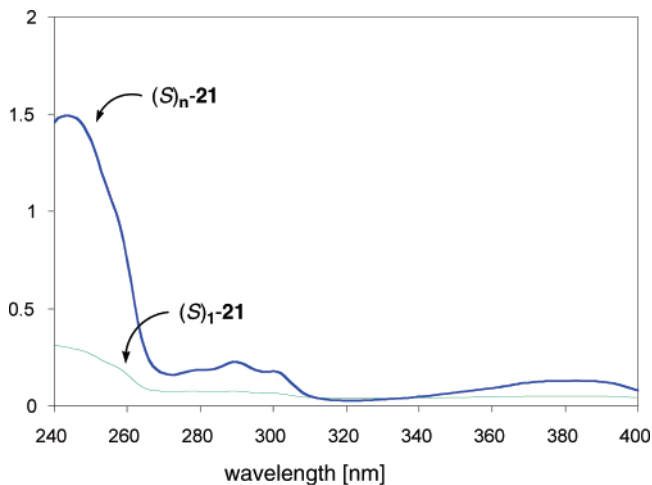


FIGURE 9. UV spectra of 2×10^{-5} M (*S*)₁-**21** and (*S*)_n-**21** in CH_2Cl_2 at ambient temperature.

Tandem Strategy with Highly Functionalized Substrates.

In further work, we studied whether a similar strategy could be executed to generate highly functionalized versions of these polymers. To this end, 7-bromonaphthalene **25** was efficiently prepared from the corresponding phenyl acetic acid (Scheme 5).²¹

(21) Mulrooney, C. A.; Xiaolin, L.; DiVirgilio, E. S.; Kozlowski, M. *C. J. Am. Chem. Soc.* **2003**, *125*, 6856–6857.

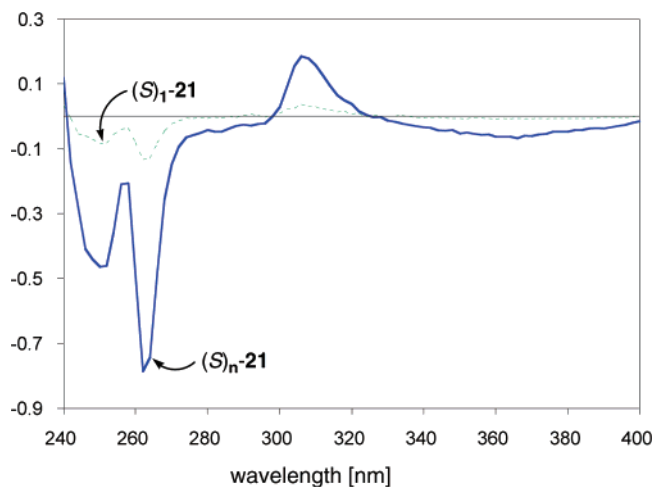
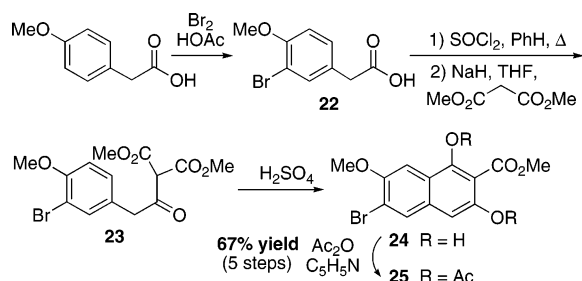
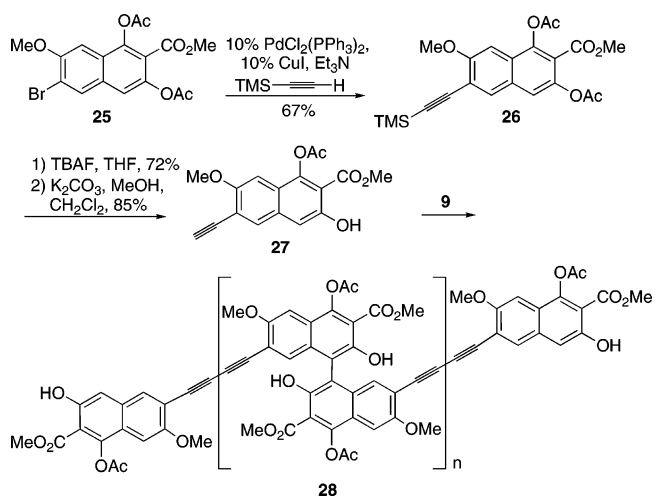


FIGURE 10. CD spectra of 2×10^{-5} M $(S)_1$ -**21** and $(S)_n$ -**21** in CH_2Cl_2 at ambient temperature.

SCHEME 5. Synthesis of a Highly Functionalized Naphthol



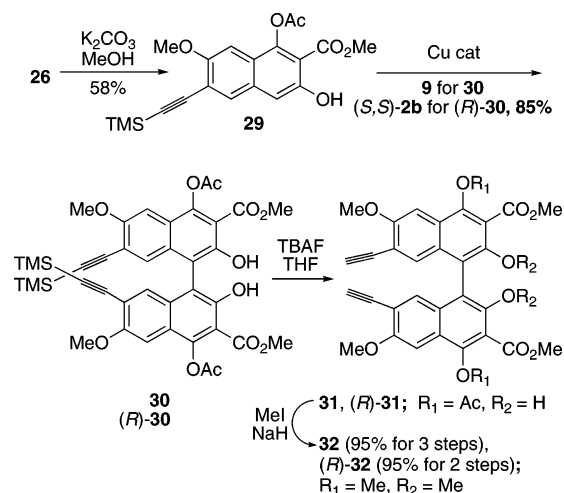
SCHEME 6. Tandem Oxidative Coupling/Glaser–Hay Coupling to Generate Polynaphthols with 1,1'- and 7,7'-linkages



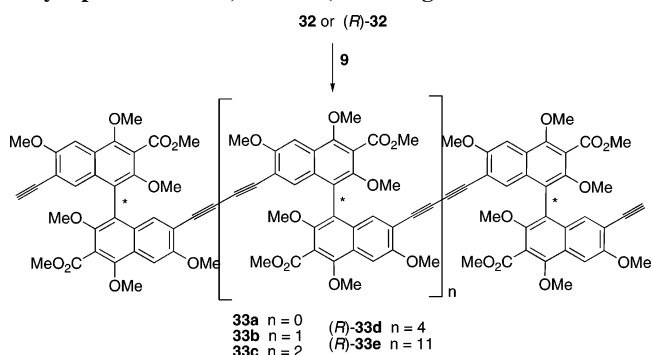
Precursor **27** was synthesized from **25** via Sonogashira coupling, silyl deprotection, and selective C2-acetate cleavage (Scheme 6). Initial attempts to affect the oxidative biaryl coupling in tandem with Glaser–Hay coupling produced **28** as an insoluble, yellow precipitate.

Because of the intractable nature of **28**, the two copper-catalyzed procedures were undertaken in a stepwise manner. Since solubilization was planned by alkylation of the phenols, the biaryl coupling was undertaken first, as the free phenol is needed for this oxidative coupling. Thus, the protected alkyne **29**, which cannot undergo the Glaser–Hay coupling, was subjected

SCHEME 7. Formation of a Chiral 1,1'-Binaphthalene with 7,7'-Cross-Linking Groups



SCHEME 8. Glaser–Hay Coupling To Generate Polynaphthols with 1,1'- and 7,7'-Linkages



to the achiral and chiral copper catalysts to afford racemic **30** and (R)-**30**, respectively (Scheme 7). Though previously the CuBF_4 catalyst was found to be more reactive and as selective as the CuI catalyst, the same reactivity pattern did not follow for this substrate. The enantioselective coupling of the highly functionalized naphthol using the CuI catalyst gave 85% yield and 82% ee as compared to 35% yield and 64% ee with the CuBF_4 catalyst. In a one-pot sequence after coupling, the alkynyl silyl group was cleaved, the phenolic acetates were hydrolyzed, and the phenols were methylated to furnish polymerization precursor **32** (Scheme 7).

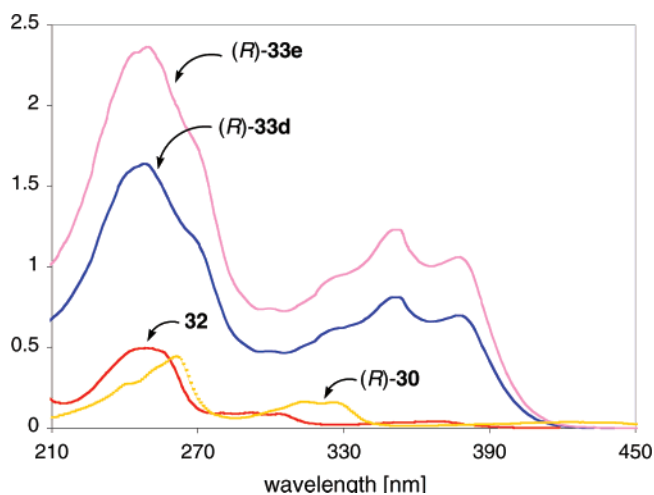
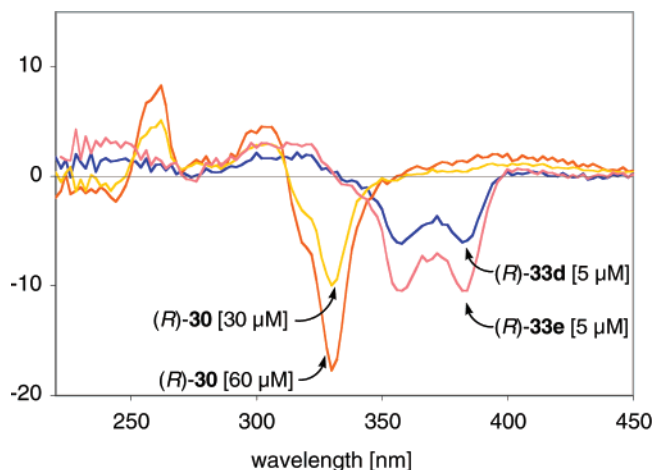
Upon treatment of **32** with the $\text{CuCl}\cdot\text{TMEDA}$ catalyst (**9**), the polymerization was affected by the Glaser–Hay coupling of terminal aryl alkynes (Scheme 8). In order to isolate lower molecular weight polymers, the polymerization of the racemic biaryl was stopped after 17 h, and the resultant materials were characterized.

The number-average molecular weights M_n from integration of the NMR signals for the terminal alkynes and the methyl ethers correlate with the data from matrix-assisted laser desorption/ionization time-of-flight (MALDI-TOF) spectrometry analysis (Table 3), indicating that cyclic species are not predominant. To achieve a higher degree of polymerization, (R)-**32** was subjected to the copper catalyst for 4 d. Because of the broadening of the signals as the polymer size increased, an accurate weight could not be determined for the chiral polymers (R)-**33d** and (R)-**33e** from NMR integration, but the M_n was established using MALDI-TOF (Table 3). MALDI-TOF was

TABLE 3. Materials Obtained from Glaser–Hay Reaction of **32** and (*R*)-**32**

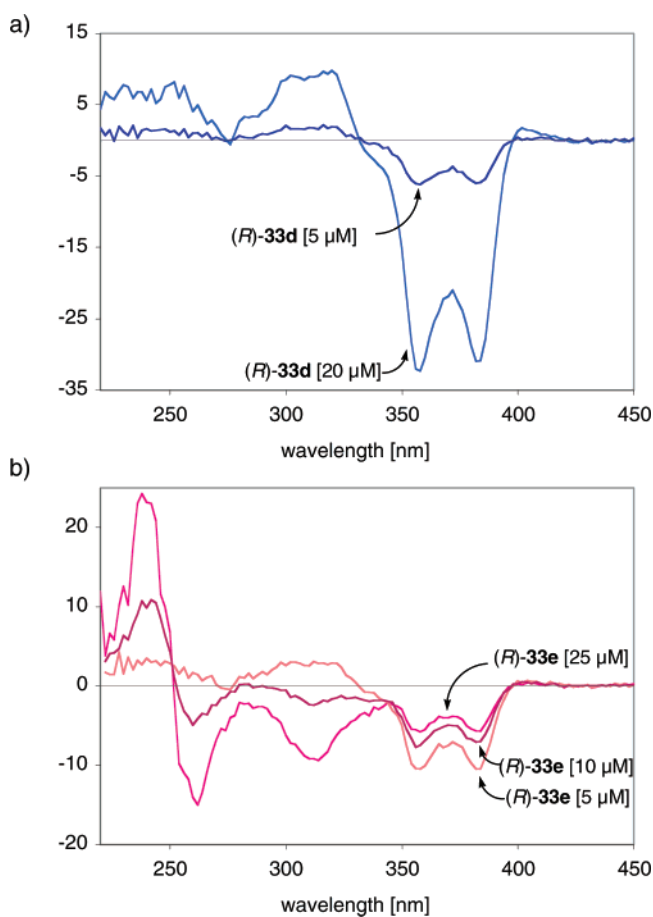
entry	product	yield (%)	M_n (NMR)	M_n (GPC) ^a	M_w/M_n (GPC)	M_n (MALDI)	$[\alpha]_D^{20}$
1	dimer 33a	15	1195	710	1.1	1219 (MNa ⁺)	
2	trimer 33b	5	1792	1160	1.1	1887 (MNa ⁺ ·THF)	
3	tetramer 33c	32	2388	1780	1.3	2387	
4	(<i>R</i>)- 33d	38	2390	2390	1.6	3623 (MK ⁺)	-708
5	(<i>R</i>)- 33e	45	6770	6770	1.6	7786 (MNa ⁺)	-1135

^a Measured by gel permeation chromatography (GPC) using a polystyrene standard.

**FIGURE 11.** UV spectra of 5 μM (*R*)-**30**, **32**, (*R*)-**33d**, (*R*)-**33e** in THF at ambient temperature.**FIGURE 12.** CD spectra of (*R*)-**30**, (*R*)-**33d**, (*R*)-**33e** in THF at ambient temperature.

accurate with the racemic polymers, and the chiral MALDI-TOF data correlated with the GPC data in the same manner as the racemic polymers.

To our surprise, the functionalized chiral polymers (*R*)-**33d** and (*R*)-**33e** gave much higher optical rotations (Table 3) in comparison to the unfunctionalized polymers described in the preceding sections. On a per binaphthyl basis, the optical rotations are also much higher than that of the corresponding binaphthyl monomer (*R*)-**30** ($[\alpha]_D^{20} -40.0$) indicating some type of higher order structure. To investigate this possibility further, the UV and CD spectra were measured. The UV spectra (Figure 11) of the binaphthols (*R*)-**30** and **32** are similar as are those of the chiral polymers (*R*)-**33d** and (*R*)-**33e**. The most

**FIGURE 13.** Concentration dependence in the CD spectra in THF at ambient temperature: (a) (*R*)-**33d**; (b) (*R*)-**33e**.

notable feature in going from the binaphthols to the chiral polymers is a shift in the longer wavelength region from 320 nm to 355/380 nm. These same differences are observed in the CD spectra (Figure 12). Under dilute conditions (5 μM), the CD spectra of chiral polymers (*R*)-**33d** and (*R*)-**33e** are identical except for their intensity due to the greater number of binaphthyl units in (*R*)-**33e**. Furthermore, the CD spectra of the shorter polymer (*R*)-**33d** (6 binaphthol units) exhibit a linear dependence upon concentration (Figure 13a). However, the CD spectra of the longer polymer (*R*)-**33e** (13 binaphthol units) vary nonlinearly with concentration (Figure 13b). In particular, the negative Cotton effects at 355 and 380 nm decrease as the concentration increases. Also, at 310 nm there is a switch from a positive Cotton effect at 5 μM to a negative Cotton effect at 10 and 25 μM . These data indicate additional structuring at higher concentrations that is consistent with aggregation of the longer polymer (*R*)-**33e** under these conditions.

Concluding Remarks

In conclusion, we report the full results from the first enantioselective approach to functionalized *chiral* polybinaphthyls from achiral starting materials. Chiral copper catalysts effect enantioselective oxidative biaryl coupling and tandem Glaser–Hay/enantioselective oxidative biaryl coupling of 2-naphthols. Since the functional group tolerance is high,²² a large number of structures are accessible using this method. This concept was demonstrated with the synthesis of highly functionalized polybinaphthyls. The CD and UV spectra of the functionalized polybinaphthyls support the formation of chiral polybinaphthyls, with different linking units giving rise to different overall structures. The relative reaction rates of various substrates with the chiral catalysts follows the order: benzyl cyanides²³ \gg aryl alkynes²⁰ > electron-rich 2-naphthols > electron-deficient 2-naphthols > alkyl alkynes.²⁰ Since the chemoselectivity of each coupling is remarkably high, substrates can be selected which assemble in a defined order under a single set of reaction conditions exposing selected terminal groups, allowing selective cross-linking, or generating more complex architectures.

Experimental Section

For general procedures as well as preparation of catalysts and monomers, see the Supporting Information.

Polymer(dihexyl 6,6'-dihydroxy-2,2'-binaphthalene-7,7'-dicarboxylate (11a and 11b)). A mixture of **8** (0.108 g, 0.2 mmol) and CuCl(OH)TMEDA (0.005 g, 0.02 mmol) in CH₂Cl₂ (2 mL) was stirred at 40 °C under O₂ for 5 d. The mixture was concentrated to give a brown solid which was washed with MeOH and then chromatographed (CH₂Cl₂) to give **11a** (0.04 g) in 37% yield as yellow crystals. The silica gel from the column was then extracted with CH₂Cl₂ and concentrated to give **11b** (0.027 g) in 25% yield as orange crystals. **11a**: GPC (THF, polystyrene standard) $M_w = 4,800$, $M_n = 3,100$, PDI = 1.6; ¹H NMR (500 MHz, CDCl₃, 4.5:1 of two sets of peaks) δ_1 (internal) 0.91–0.95 (m, 6H), 1.41–1.54 (m, 12H), 1.85–1.90 (m, 4H), 4.44–4.47 (m, 4H), 7.31–7.34 (m, 2H), 7.69–7.73 (m, 2H), 8.19–8.24 (m, 2H), 8.75–8.77 (m, 2H), 10.88–10.90 (m, 2H); δ_2 (terminal) 0.91–0.95 (m, 6H), 1.41–1.54 (m, 12H), 1.85–1.90 (m, 4H), 4.09 (br, 4H), 7.34 (s, 2H), 7.79 (d, $J = 8.6$ Hz, 2H), 7.87 (d, $J = 8.2$ Hz, 2H), 8.10 (s, 2H), 8.56 (s, 2H) 10.57 (s, 2H); ¹³C NMR (125 MHz, CDCl₃) δ_1 (internal) 14.0, 22.53, 25.67, 28.59, 31.43, 66.12, 115.0, 116.9, 125.4, 126.8, 127.5, 129.0, 133.0, 136.0, 136.3, 154.5, 170.1; δ_2 (terminal) 13.96, 22.50, 25.64, 28.54, 31.40, 65.95, 115.0, 111.6, 127.0, 127.3, 127.5, 128.95, 132.5, 135.95, 137.0, 156.7, 169.9; IR (film) 3206, 2929, 1677 cm⁻¹; Elemental analysis (C₃₄H₃₈O₆) calcd C 75.25, H 7.06, found C 75.44, H 6.92. **11b**: GPC (THF, polystyrene standard) $M_w = 8,500$, $M_n = 5,800$, PDI = 1.5; ¹H NMR and ¹³C NMR spectra are similar to those of **11a**.

Polymer (S)_n-11c. To a mixture of **8** (0.054 g, 0.10 mmol) in CH₂Cl₂ (1 mL) was added the CuI(*R,R*)-1,5-diaza-*cis*-decalin catalyst (0.003 g, 0.01 mmol). After being stirred at 40 °C under O₂ for 4 d, the mixture was concentrated to give a brown solid which was washed with MeOH. Chromatography (7.5% EtOAc/hexanes, then CH₂Cl₂) provided (S)-**11c** (0.028 g) in 52% yield as yellow crystals: $[\alpha]_D^{25} +82$ (c 1.4, CHCl₃); GPC (THF, polystyrene standard) $M_w = 2,800$, $M_n = 2,200$, PDI = 1.3; ¹H NMR spectrum is similar to that of **11a**.

Polymer (S)_n-11d. To a mixture of **8** (0.054 g, 0.10 mmol) in ClCH₂CH₂Cl (2 mL) and DMF (0.05 mL) was added the CuBF₄(*R,R*)-1,5-diaza-*cis*-decalin catalyst (0.006 g, 0.02 mmol). The resultant solution was stirred at 60 °C for 5 d and then cooled to room temperature. After removal of the solvent, the resultant solid was washed with MeOH to remove the catalyst. The dried solid was dissolved in CH₂Cl₂ and precipitated with MeOH. This procedure was repeated three times. After removal of trace solvent *in vacuo*, the remaining material consisted of **11d** which was obtained as a yellow solid in 74% (0.040 g) yield: $[\alpha]_D^{25} +78$ (c 0.13, CH₂Cl₂); GPC (THF, polystyrene standard) $M_w = 10,600$, $M_n = 4,900$ (PDI = 2.2); UV-vis(CH₂Cl₂) λ_{max} 325 nm; ¹H NMR and ¹³C NMR spectra are similar to those of **11a**.

Dimer 11e and Trimer 11f. These materials were obtained by halting the reaction prior to completion. To a mixture of **8** (0.054 g, 0.10 mmol) in ClCH₂CH₂Cl (2 mL) was added CuCl(OH)-TMEDA (0.046 g, 0.02 mmol). The resultant mixture was stirred at 60 °C for 1 h. After removal of the solvent, the residue was chromatographed (50–80% CH₂Cl₂/hexanes) which provided recovered **8** (0.022 g, 41%), **11e** (0.015 g, 28%), and **11f** (0.005 g, 9%).

Dimer 11e. ¹H NMR (500 MHz, CDCl₃) δ 0.91–0.97 (m, 12H), 1.25–1.54 (m, 24H), 1.85–1.90 (m, 8H), 4.42–4.51 (m, 8H), 7.33–7.35 (m, 4H), 7.74 (dd, $J = 8.9$, 1.8 Hz, 2H), 7.79 (d, $J = 8.7$ Hz, 2H), 7.87 (dd, $J = 8.7$, 1.8 Hz, 2H), 8.09 (s, 2H), 8.25 (d, $J = 1.4$ Hz, 2H), 8.55 (s, 2H), 8.79 (s, 2H), 10.58 (s, 2H), 10.92 (s, 2H); ¹³C NMR (125 MHz, CDCl₃) δ 14.0, 14.1, 22.5, 22.6, 25.6, 25.7, 28.5, 28.6, 31.4, 31.5, 66.0, 66.2, 111.6, 114.8, 114.9, 116.8, 125.5, 126.9, 127.0, 127.3, 127.5, 128.7, 129.0, 132.5, 132.9, 135.3, 135.8, 136.1, 136.3, 137.0, 154.4, 156.5, 169.8, 170.1; IR (film) 3206, 2929, 1677 cm⁻¹; Elemental analysis (C₆₈H₇₄O₁₂) calcd C 75.39, H 6.89, found C 75.85, H 7.27.

Trimer 11f. ¹H NMR (500 MHz, CDCl₃) δ 0.92–0.95 (m, 18H), 1.38–1.53 (m, 36H), 1.85–1.89 (m, 12H), 4.42–4.50 (m, 12H), 7.31–7.34 (m, 6H), 7.70–7.74 (m, 4H), 7.78 (d, $J = 8.7$ Hz, 2H), 7.86 (dd, $J = 8.7$, 1.7 Hz, 2H), 8.08 (s, 2H), 8.22 (d, $J = 1.7$ Hz, 1H), 8.23 (d, $J = 1.7$ Hz, 1H), 8.24 (d, $J = 1.5$ Hz, 2H), 8.54 (s, 2H), 8.76 (s, 1H), 8.77 (s, 1H), 8.78 (s, 2H), 10.57 (s, 2H), 10.90 (s, 4H); ¹³C NMR (125 MHz, CDCl₃) δ 13.99, 14.02, 22.52, 22.56, 25.66, 25.70, 28.56, 28.62, 31.44, 31.48, 66.00, 66.18, 111.6, 115.0 (2C), 116.9, 125.4, 126.9, 127.0, 127.3, 127.5, 128.7, 129.0, 129.1, 132.5, 133.0, 136.0, 136.1, 136.3, 136.8, 154.5, 156.7, 169.9, 170.2; IR (film) 3206, 2929, 1677 cm⁻¹; Elemental analysis (C₁₀₂H₁₁₀O₁₈) calcd C 75.44, H 6.83, found C 75.63, H 7.19.

Dimer (R)-11e and Trimer (R,R)-11f. These materials were obtained by halting the reaction prior to completion. To a mixture of **8** (0.054 g, 0.1 mmol) in ClCH₂CH₂Cl (2 mL) and DMF (0.05 mL) was added the CuBF₄(*S,S*)-1,5-diaza-*cis*-decalin catalyst (0.006 g, 0.02 mmol). The resultant mixture was stirred at 60 °C for 3 h. After removal of the solvent, the residue was chromatographed (50–80% CH₂Cl₂/hexanes) which provided recovered **8** (0.025 g, 46%), **11e** (0.017 g, 31%), and **11f** (0.004 g, 7%).

Dimer (R)-11e. $[\alpha]_D^{25} -60$ (c 0.05, CH₂Cl₂); UV-vis (CH₂Cl₂) λ_{max} 270 nm; ¹H NMR spectrum is the same as that of **11e** (see above).

Trimer (R,R)-11f. $[\alpha]_D^{25} -71$ (c 0.095, CH₂Cl₂); UV-vis (CH₂Cl₂) λ_{max} 270 nm; ¹H NMR δ 0.92–0.95 (m, 18H), 1.38–1.53 (m, 36H), 1.85–1.89 (m, 12H), 4.42–4.50 (m, 12H), 7.27–7.34 (m, 6H), 7.70–7.74 (m, 4H), 7.78 (d, $J = 8.7$ Hz, 2H), 7.86 (dd, $J = 8.7$, 1.8 Hz, 2H), 8.08 (s, 2H), 8.22 (d, $J = 1.7$ Hz, 0.3H), 8.23 (d, $J = 1.7$ Hz, 1.7H), 8.24 (d, $J = 1.7$ Hz, 2H), 8.54 (s, 2H), 8.76 (s, 0.5H), 8.77 (s, 1.5H), 8.78 (s, 2H), 10.57 (s, 2H), 10.90 (s, 4H).

(R)_n-17a from Glaser Coupled Bisalkyne 16. To a mixture of **16** (0.059 g, 0.1 mmol) in ClCH₂CH₂Cl (2 mL) and DMF (0.05 mL) was added the CuBF₄(*S,S*)-1,5-diaza-*cis*-decalin catalyst (0.012 g, 0.04 mmol). The resultant mixture was stirred at 80 °C for 2 d. After removal of the solvent, the residue was chromatographed (10% MeOH/CH₂Cl₂) to yield a solid which was precipitated with

(22) Xiaolin, L.; Hewgley, J. B.; Mulrooney, C. A.; Yang, J.; Kozlowski, M. C. *J. Org. Chem.* **2003**, *68*, 5500–5511.

(23) Our copper complex **2b** catalyzes the benzyl cyanide couplings described by de Jongh in ~5 min at -78 °C: de Jongh, H. A. P.; de Jongh, R. H. I.; Mijs, W. J. *J. Org. Chem.* **1971**, *36*, 3160–3168.

MeOH to afford (*R*)-**17a** as a yellow solid in 90% yield: $[\alpha]_D^{25}$ -248 (*c* 0.1, CH₂Cl₂); GPC (THF, polystyrene standard) $M_w = 12\,900$, $M_n = 4400$, PDI = 2.9; ¹H NMR (500 MHz, CDCl₃, 6:1 ratio of two sets of peaks) δ_1 (internal) 0.89–0.96 (m, 6H), 1.30–1.52 (m, 12H), 1.84–1.89 (m, 4H), 4.42–4.47 (m, 4H), 7.10 (d, *J* = 8.9 Hz, 2H), 7.40 (d, *J* = 8.6 Hz, 2H), 8.14 (s, 2H), 8.63 (s, 2H), 10.98 (s, 2H); δ_2 (terminal) 7.29 (s, 2H), 7.54 (d, *J* = 8.6 Hz, 2H), 7.64 (d, *J* = 8.5 Hz, 2H), 8.05 (s, 2H), 8.44 (s, 2H), 10.68 (s, 2H); ¹³C NMR (125 MHz, CDCl₃) δ_1 (internal) 14.0, 22.5, 25.6, 28.5, 31.4, 66.3, 74.5, 81.8, 115.3, 116.8, 117.2, 124.9, 126.6, 131.8, 132.8, 134.8, 136.7, 155.5, 169.8; small peaks from the termini were observed at δ_2 (terminal) 66.1, 74.4, 81.8, 112.0, 117.0, 124.8, 126.4, 126.7, 131.4, 132.2, 134.3, 137.5, 155.7, 169.6; IR (film) 2929, 1680 cm⁻¹; Elemental analysis (C₃₈H₃₈O₆) calcd C 77.27, H 6.48, found C 75.69, H 5.06.

(*R*)-17b** from Monomer **14**.** To a mixture of **14** (0.059 g, 0.2 mmol) in ClCH₂CH₂Cl (2 mL) and DMF (0.05 mL) was added the CuBF₄(*S,S*)-1,5-diaza-*cis*-decalin catalyst (0.012 g, 0.04 mmol). The resultant mixture was stirred at 80 °C for 2 d. After removal of the solvent, the residue was chromatographed (10% MeOH/CH₂Cl₂) to yield a solid which was precipitated with MeOH to afford **17b** as a yellow solid in 80% yield: $[\alpha]_D^{25}$ -168 (*c* 0.1, CH₂Cl₂); GPC (THF, polystyrene standard) $M_w = 9200$, $M_n = 4900$, PDI = 1.9; ¹H NMR and ¹³C NMR are similar to those of (*R*)-**17a** obtained from bisalkyne **16**.

(*S*)-17c** from Dimer (*S*)-**19**.** To a solution of **19** (59 mg, 0.1 mmol) in ClCH₂CH₂Cl (2 mL) was added CuCl(OH)TMEDA (2 mg, 0.01 mmol). The resultant mixture was stirred at 80 °C under O₂ for 2 d. After removal of the solvent, the residue was precipitated **17c** as a yellow resin (51 mg) in 86% yield: $[\alpha]_D^{25}$ 238 (*c* 0.08, CH₂Cl₂); GPC (THF, polystyrene standard) $M_w = 11\,000$, $M_n = 5100$, PDI = 2.2; ¹H NMR (500 MHz, CDCl₃) δ 0.93–0.96 (m, 6H), 1.40–1.52 (m, 12H), 1.85–1.90 (m, 4H), 4.45–4.48 (m, 4H), 7.10 (d, *J* = 8.8 Hz, 2H), 7.39 (d, *J* = 9.0 Hz, 2H), 8.16 (s, 2H), 8.62 (s, 2H), 10.96 (m, 2H); ¹³C NMR (125 MHz, CDCl₃) δ 14.0, 22.5, 25.7, 28.6, 31.4, 66.3, 74.5, 81.9, 115.3, 116.9, 117.3, 124.9, 126.6, 131.8, 132.8, 134.8, 136.7, 155.5, 169.8; Elemental analysis (C₃₈H₃₆O₆) calcd C 77.53, H 6.16, found C 76.35, H 5.87.

(*S*)-21**.** To a mixture of **15** (0.120 g, 0.45 mmol) in 1,2-dichloroethane (4 mL) and DMF (0.05 mL) was added catalyst (*R,R*)-**2d**. After being stirred at 70 °C for 4 d under O₂, the mixture was cooled and concentrated. The residue was washed with MeOH to remove the catalyst, and the residual solvent was removed in vacuo. The resultant solid was dissolved in CH₂Cl₂ and precipitated with MeOH. This procedure was repeated three times to provide an orange solid (0.072 g) in 60% yield: $[\alpha]_D^{25}$ -180 (*c* 0.05, CH₂Cl₂); GPC (THF, polystyrene standard) $M_w = 10\,300$, $M_n = 3900$, PDI = 2.6; ¹H NMR (500 MHz, CDCl₃) δ 1.76–1.78 (m, 2H), 2.00 (br, 2H), 2.40–2.41 (m, 2H), 4.46 (br, 2H), 7.25–7.16 (m, 1H), 7.31 (br, 2H), 7.93 (br, 1H), 8.67 (s, 1H), 10.75 (s, 1H); ¹³C NMR (125 MHz, CDCl₃) δ 18.9, 24.9, 27.7, 65.3, 66.0, 76.9, 114.2, 117.0, 123.9, 124.7, 127.2, 129.4, 132.7, 137.2, 154.1, 170.1; IR (CHCl₃ solution) 1678, 1280 cm⁻¹; Elemental analysis (C₃₄H₃₀O₆) calcd C 76.67, H 5.30, found C 73.40, H 5.04.

(*R*)-Dimethyl 1,1'-Diacetoxy-3,3'-dihydroxy-7,7'-dimethoxy-6,6'-(di-2-(trimethylsilyl)ethynyl)-1,1'-binaphthalene-2,2'-dicarboxylate ((*R*)-30**).** To a solution of **29** (200 mg, 0.52 mmol) in CH₂Cl₂ (3 mL) and ClCH₂CH₂Cl (2 mL) was added the CuI(*S,S*)-1,5-diaza-*cis*-decalin catalyst (36 mg, 0.10 mmol). After being stirred for 3 d under oxygen, the solution was quenched with 1 N HCl. The aqueous phase was extracted with CH₂Cl₂, the organics were washed with brine and dried (Na₂SO₄), and the solvent was evaporated in vacuo. The resultant resin was chromatographed (60% EtOAc/hexanes) to give (*R*)-**30** (170 mg) as a yellow solid in 85% yield: $R_f = 0.31$ (50% EtOAc/hexanes); mp 254–257 °C; $[\alpha]_D^{20}$ -40.0 ; IR (thin film) 3177, 2961, 2922, 2853, 2154, 1776, 1675, 1621, 1571 cm⁻¹; ¹H NMR (500 MHz, CDCl₃) δ 0.08 (s, 18H), 2.54 (s, 6H), 3.96 (s, 6H), 4.03 (s, 6H), 7.11 (s, 2H), 7.26 (s, 2H),

10.64 (s, 2H); ¹³C NMR (125 MHz, CDCl₃) δ 169.6, 169.2, 156.5, 153.0, 147.7, 132.3, 131.0, 122.6, 119.2, 115.1, 108.8, 102.1, 100.7, 100.5, 56.2, 53.5, 21.3, 0.2; HRMS (ESI) calcd for C₄₀H₄₂O₁₂Si₂ (MNa⁺) 793.2100, found 793.2098; CSP HPLC (Chiralpak AD, 1.0 mL/min, 90:10 hexanes:*i*-PrOH) t_R (*R*) = 8.1 min, t_R (*S*) = 12.5 min; 82% ee.

Dimethyl 1,1',3,3',7,7'-Hexamethoxy-6,6'-diethynyl-1,1'-binaphthalene-2,2'-dicarboxylate (32**).** To a solution of **30** in THF (4 mL) was added TBAF (0.34 mL, 0.34 mmol). After being stirred for 15 min at room temperature under argon, the solvent was evaporated in vacuo. The resultant brown solid was dissolved in EtOAc and washed with brine. The organics were dried, and the solvent was evaporated in vacuo. The yellow solid, **31**, was carried on to the next step without further purification.

To a solution of **31** in DMF (5 mL) were added NaH (60% in oil, 100 mg, 2.4 mmol) and MeI (0.35 mL, 5.1 mmol). After being stirred for 4 h at room temperature under argon, the mixture was quenched with 1 N HCl. The aqueous phase was extracted with EtOAc, and the combined organics were washed with 1 N HCl (3 × 20 mL) and brine (2 × 20 mL). The organics were dried (Na₂SO₄), and after the solvent was evaporated, the residue was chromatographed (50% EtOAc/hexanes) to give **32** as a clear resin (95 mg) in 95% yield over the three steps: $R_f = 0.43$ (50% EtOAc/hexanes); IR (thin film) 3285, 2945, 2926, 2853, 2108, 1733, 1590 cm⁻¹; ¹H NMR (500 MHz, CDCl₃) δ 3.26 (s, 2H), 3.35 (s, 6H), 3.99 (s, 6H), 4.04 (s, 6H), 4.14 (s, 6H), 7.30 (s, 2H), 7.48 (s, 2H); ¹³C NMR (125 MHz, CDCl₃) δ 167.1, 157.4, 153.6, 152.2, 132.5, 129.8, 126.2, 121.8, 119.6, 115.4, 101.1, 82.8, 79.9, 62.9, 62.3, 56.3, 53.0; HRMS (ESI) calcd for C₃₄H₃₀O₁₀ (MNa⁺) 621.1700, found 621.2802.

(*R*)-Dimethyl 1,1',3,3',7,7'-Hexamethoxy-6,6'-diethynyl-1,1'-binaphthalene-2,2'-dicarboxylate ((*R*)-32**).** (*R*)-**31** was prepared in the same manner as **31** above and was obtained as a yellow solid and carried on to the next step without further purification.

(*R*)-**32** was prepared in the same way as **32** and was obtained as a clear resin in 95% yield. ¹H NMR and ¹³C NMR are similar to those of **32**.

Dimer **33a, Trimer **33b**, and Tetramer **33c**.** These materials were obtained by halting the reaction prior to completion. To a mixture of **32** (0.095 g, 0.16 mmol) in CH₂Cl₂ (5 mL) was added CuCl(OH)TMEDA (0.008 g, 0.032 mmol). The resultant mixture was stirred at room temperature for 17 h under an oxygen atmosphere. The reaction was quenched with 1 N HCl, and the aqueous phase was extracted with CH₂Cl₂. The organics were dried (Na₂SO₄), and after the solvent was evaporated, the residue was chromatographed (50–80% EtOAc/hexanes) to yield **33a** (0.015 g, 16%), **33b** (0.005 g, 5%), and **33c** (0.030 g, 32%).

Dimer **33a.** $R_f = 0.08$ (50% EtOAc/hexanes); $M_{n,NMR} = 1195$, $M_{n,GPC} = 710$, $M_w/M_n = 1.1$, $M_{n,MALDI-TOF} = 1219$ (MNa⁺); ¹H NMR (500 MHz, CDCl₃) δ 3.23 (s, 2H), 3.34 (s, 6H), 3.36 (s, 6H), 3.98 (s, 6H), 3.99 (s, 12H), 4.04 (s, 6H), 4.12 (s, 6H), 4.15 (s, 6H), 7.26 (s, 2H), 7.28 (s, 2H), 7.43 (s, 2H), 7.48 (s, 2H); ¹³C NMR (125 MHz, CDCl₃) δ 166.8, 166.7, 157.5, 157.2, 153.5, 153.3, 152.0, 151.9, 132.9, 132.1, 129.6, 129.5, 126.1, 126.0, 121.6, 119.3, 119.2, 115.2, 114.9, 100.9, 100.7, 82.4, 79.7, 79.0, 78.7, 62.7, 62.6, 62.0, 61.9, 56.1, 56.0, 52.7, 52.6; IR (film) 3277, 2926, 2853, 2212, 1733, 1590 cm⁻¹

Trimer **33b.** $R_f = 0.17$ (2.5% MeOH/CH₂Cl₂); $M_{n,NMR} = 1792$, $M_{n,GPC} = 1160$, $M_w/M_n = 1.1$, $M_{n,MALDI-TOF} = 1887$ (MNa⁺;THF); ¹H NMR (500 MHz, CDCl₃) δ 3.23 (br s, 2H), 3.33 (s, 6H), 3.35 (s, 3H), 3.34 (s, 3H), 3.35 (s, 6H), 3.97 (s, 6H), 3.98 (s, 6H), 3.99 (s, 18H), 4.03 (s, 3H), 4.04 (s, 3H), 4.12 (s, 6H), 4.13 (s, 6H), 4.14 (s, 6H), 7.23 (s, 2H), 7.25 (s, 1H), 7.25 (s, 1H), 7.28 (s, 2H), 7.42 (s, 2H), 7.43 (s, 2H), 7.48 (s, 2H); ¹³C NMR (125 MHz, CDCl₃) δ 166.8, 166.7, 166.6, 157.5, 157.4, 157.2, 153.4, 153.3, 152.0, 151.9, 132.9, 132.8, 132.1, 129.6, 129.5, 126.2, 126.0, 121.6, 119.3, 119.2, 115.2, 115.0, 114.9, 100.9, 100.8, 82.4, 79.7, 79.1, 79.0, 78.7, 78.6, 62.7, 62.6, 62.0, 61.9, 56.0, 55.9, 52.7, 52.6; IR (film) 3296, 2961, 2926, 2853, 2212, 1729, 1590 cm⁻¹

Tetramer 33c. $R_f = 0.14$ (2.5% MeOH/CH₂Cl₂); $M_{n,NMR} = 2388$, $M_{n,GPC} = 1780$, $M_w/M_n = 1.3$, $M_{n,MALDI-TOF} = 2387$; ¹H NMR (500 MHz, CDCl₃) δ 3.23 (s, 2H), 3.33 (br s, 18H), 3.35 (s, 6H), 3.98 (br m, 42H), 4.02 (br s, 6H), 4.12 (br m, 24H), 7.21 (br m, 6H), 7.25 (br s, 2H), 7.42 (br m, 6H), 7.47 (br s, 2H); ¹³C NMR (125 MHz, CDCl₃) δ 167.1, 167.0, 166.9, 157.8, 157.4, 153.7, 153.7, 153.5, 152.3, 152.2, 152.2, 133.1, 133.0, 132.3, 129.9, 129.8, 129.8, 126.4, 126.3, 126.3, 122.1, 122.1, 121.8, 119.6, 119.5, 119.5, 115.5, 115.2, 101.1, 101.0, 82.7, 80.0, 79.4, 78.9, 63.0, 62.2, 56.3, 52.8; IR (film) 3293, 2999, 2949, 2845, 2212, 1733, 1590 cm⁻¹.

(R)-33. To a mixture of **(R)-32** (0.080 g, 0.13 mmol) in CH₂Cl₂ (3 mL) was added CuCl(OH)TMEDA (0.006 g, 0.027 mmol). The resultant mixture was stirred at room temperature for 4 d under an oxygen atmosphere. The reaction was quenched with 1 N HCl, and the aqueous phase was extracted with CH₂Cl₂. The organics were dried (Na₂SO₄), and after the solvent was evaporated, the residue was chromatographed (1–10% MeOH/CH₂Cl₂) to yield **(R)-33d** (30 mg, 38%) and **(R)-33e** (36 mg, 45%) as the main fractions.

(R)-33d. $R_f = 0.11$ (2.5% MeOH/CH₂Cl₂); $M_{n,GPC} = 2390$, $M_w/M_n = 1.6$, $M_{n,MALDI-TOF} = 3623$ (MK⁺); $[\alpha]_D^{20} -707.8$; ¹H NMR (500 MHz, CDCl₃) δ 3.33 (br s, 6H), 3.97 (br s, 12H), 4.12 (br m, 6H), 7.22 (br m, 2H), 7.42 (br m, 2H); ¹³C NMR (125 MHz, CDCl₃) δ 166.9, 157.8, 153.6, 152.2, 133.0, 129.8, 126.4, 122.1, 119.5,

115.3, 101.1, 79.4, 79.0, 62.9, 62.2, 56.2, 52.8; IR (film) 3204, 2926, 2853, 2212, 1733, 1586 cm⁻¹.

(R)-33e. $R_f = 0.09$ (2.5% MeOH/CH₂Cl₂); $M_{n,GPC} = 6770$, $M_w/M_n = 1.6$, $M_{n,MALDI-TOF} = 7786$ (MNa⁺); $[\alpha]_D^{20} -1135.0$; ¹H NMR (500 MHz, CDCl₃) δ 3.32 (br s, 6H), 3.97 (br s, 12H), 4.11 (br m, 6H), 7.21 (br m, 2H), 7.42 (br m, 2H); ¹³C NMR (125 MHz, CDCl₃) δ 166.6, 157.5, 153.4, 151.9, 132.7, 129.5, 126.1, 121.8, 119.2, 115.0, 100.9, 79.1, 78.6, 62.7, 61.9, 56.0, 52.6; IR (film) 3204, 2999, 2926, 2853, 2212, 1733, 1586 cm⁻¹.

Acknowledgment. Financial support was provided by the University of Pennsylvania Research Foundation, the National Science Foundation (CHE-0616885), and the National Institutes of Health (CA-109164). We thank Andres Dulcey, Jonathon Ruddick, Janine Ladislav, and Prof. Virgil Percec for assistance with the polymer characterization.

Supporting Information Available: Experimental details and characterization of all new compounds. This material is available free of charge *via* the Internet at <http://pubs.acs.org>.

JO070636+